

Electron beams in asymmetric capacitively coupled radio frequency discharges at low pressures

This article has been downloaded from IOPscience. Please scroll down to see the full text article.

2008 J. Phys. D: Appl. Phys. 41 042003

(<http://iopscience.iop.org/0022-3727/41/4/042003>)

View [the table of contents for this issue](#), or go to the [journal homepage](#) for more

Download details:

IP Address: 38.107.179.211

The article was downloaded on 21/02/2012 at 13:17

Please note that [terms and conditions apply](#).

FAST TRACK COMMUNICATION

Electron beams in asymmetric capacitively coupled radio frequency discharges at low pressures

J Schulze¹, B G Heil¹, D Luggenhölscher¹, T Mussenbrock²,
R P Brinkmann² and U Czarnetzki¹

¹ Institute for Plasma and Atomic Physics, Ruhr-University Bochum, Germany

² Institute for Theoretical Electrical Engineering, Ruhr-University Bochum, Germany

E-mail: fjschulze@hotmail.com

Received 30 December 2007

Published 1 February 2008

Online at stacks.iop.org/JPhysD/41/042003

Abstract

The generation of directed energetic electrons by the expanding sheath is observed in asymmetric capacitively coupled radio frequency discharges at low pressures (≤ 1 Pa) in different gases. The phenomenon of such electron beams is investigated by a combination of experimental diagnostics, an analytical model and simulations. At sufficiently low pressures multiple reflections of electron beams at the plasma boundaries are observed. An analytical model shows how these beams lead to an enhanced high energy tail of the electron energy distribution function. Thus, stochastic heating is closely related to electron beams.

(Some figures in this article are in colour only in the electronic version)

Capacitively coupled radio frequency (CCRF) discharges are intensively used for etching and deposition processes as one of many steps in the production chain of integrated circuits. For industrial applications these discharges are typically operated at low pressures (≤ 1 Pa) and generally asymmetric. Despite this enormous relevance for applications, basic phenomena such as electron (stochastic) heating at low pressures are not fully understood and are an important current research topic.

Several models of stochastic heating exist [1–4]. However, only a few experimental investigations have been performed [5, 6]. In this work a detailed experimental and theoretical investigation of electron heating in asymmetric CCRF discharges, 13.56 MHz, at low pressures is performed. Various diagnostics in combination with an analytical model and numerical simulations are applied in order to get a detailed picture of electron dynamics. Cause and effect of electron heating are investigated and only the synergistic effect of different experimental diagnostics and theoretical approaches yields a better understanding of this fundamental phenomenon.

The cause of stochastic heating in terms of the spatio-temporal evolution of the electric field in the sheath

is investigated by fluorescence dip spectroscopy (FDS) in krypton [7] with high spatial ($50 \mu\text{m}$) and temporal resolution within the RF period (5 ns). The effect of electron heating is the excitation caused by energetic electrons. Phase resolved optical emission spectroscopy (PROES) is used in order to detect the excitation space and phase resolved with a resolution of $50 \mu\text{m}$ and 4.2 ns, respectively. The plasma is characterized by radially resolved Langmuir probe measurements of the electron density, the electron mean energy and the electron energy distribution function (EEDF). The measured electric fields are compared with theoretically calculated ones using a fluid sheath model [8] with experimentally obtained input parameters. The spatio-temporal excitation is calculated by a hybrid Monte Carlo simulation using the electric fields resulting from the fluid model as input parameters [9]. An analytical model [10] describes the influence of energetic electron beams on the time averaged EEDF in the bulk as measured by a Langmuir probe.

In a modified GEC reference cell (figure 1) measurements are performed in an asymmetric CCRF discharge in krypton with and without a small admixture of neon as a tracer

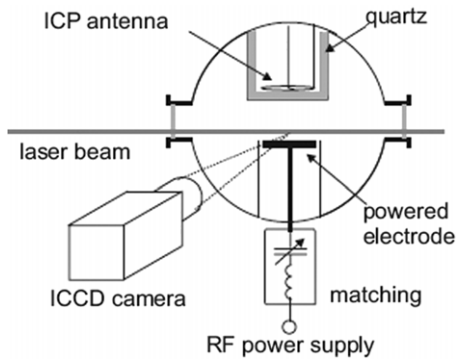


Figure 1. Experimental setup: GEC reference cell, laser beams and ICCD camera used for FDS and PROES measurements.

gas. The discharge is operated at 8 W and at low pressures (≤ 1 Pa). The chamber is a standard hybrid CCP/ICP cell and the modification is a replacement of the metal cylinder surrounding the ICP antenna by a monolithic quartz housing. For the investigations presented here the ICP antenna is not used. The electrode radius and gap between electrode and quartz are 5 cm, respectively. In order to measure the electric field in the sheath at the powered electrode two laser beams enter the discharge from the side parallel to the powered electrode [7]. The resulting laser induced fluorescence light is detected by an ICCD camera. Both lasers and the ICCD camera are synchronized with the RF voltage to allow phase resolved measurements within the RF cycle. The experimental setup and excitation scheme used for these investigations are described in detail elsewhere [7, 10]. For space and phase resolved measurements of the plasma emission a fast gateable ICCD camera (Andor iStar) is used, which is synchronized with the RF voltage. Depending on the gas mixture emission from either the Kr $2p_5$ state (11.7 eV) or the Ne $2p_1$ state (19 eV) is observed. Under the conditions investigated here the excitation can be calculated easily from the measured emission [10].

Most measurements are performed in a pure krypton discharge at 1 Pa and 8 W. At these parameters Langmuir probe measurements (Scientific Systems, Smart Probe) at the axial centre between electrode and quartz yield an electron density of $2 \times 10^9 \text{ cm}^{-3}$ and a mean energy of 5 eV.

Figure 2 shows the spatio-temporal evolution of the electric field in the sheath under these conditions as it is measured by FDS (markers) and obtained from a fluid sheath model (solid lines) [8, 10]. Good agreement between theory and experiment is found. For the model experimentally obtained input parameters for pressure, voltage, electron density and electron temperature are used and no fit is involved in figure 2. The maximum sheath width at the phase of full sheath expansion is 1 cm. The phases of sheath expansion and collapse are clearly visible. The phase of fastest sheath expansion takes place between about 5 and 20 ns. Within this time interval electrons are accelerated out of the sheath into the plasma. At 21.5 ns the sheath is already fully expanded. From these measurements voltages and profiles of charge densities in the sheath can be obtained [10].

Figure 3 (colour online) shows a contour plot of the space and phase resolved excitation into Kr $2p_5$ close to the

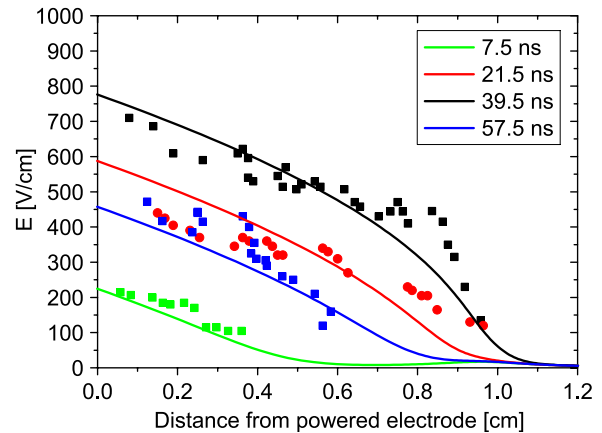


Figure 2. Spatio-temporal evolution of the electric field in the sheath. The markers are experimental (FDS) and the solid lines are theoretical results (fluid sheath model). In the experiment the temporal resolution is 5 ns. The times given here correspond to the centre of this time interval. For comparison the same temporal integration is applied in the simulation.

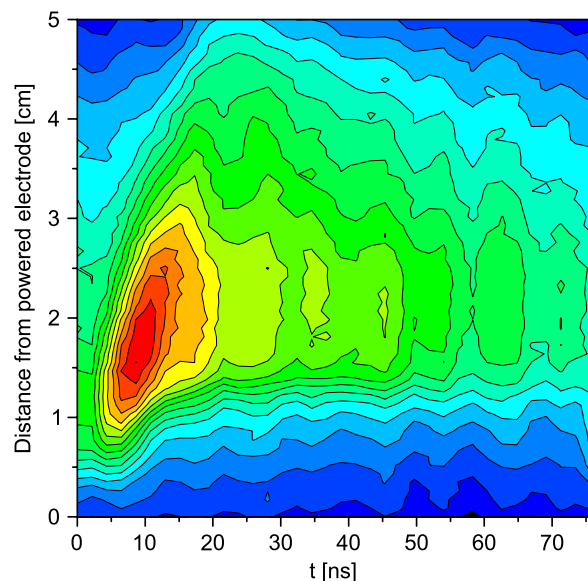


Figure 3. Spatio-temporal plot of the excitation into Kr $2p_5$ close to the powered electrode at 1 Pa in a krypton discharge. (Colour online.)

powered electrode under the same conditions. In such plots red corresponds to high and blue to low excitation. An absolute phase calibration between FDS and PROES measurements has been performed, so that the timescales in figures 2 and 3 are identical. Therefore, the effect of electron heating in terms of the propagation of energetic electrons can be directly linked to its cause.

The maximum sheath width is estimated from figure 3 to be 1 cm, which agrees well with the result of the FDS measurements. At the beginning of the RF cycle (5–20 ns), when the sheath expands at maximum velocity, the generation of a beam of energetic electrons is observed. In such spatio-temporal plots of the excitation an electron beam appears as a tilted trajectory. From the tilt of this trajectory the propagation velocity of the beam is estimated to be $2.2 \times 10^6 \text{ m s}^{-1}$ (11 eV). The term ‘beam’ is used for electrons leaving the sheath at a

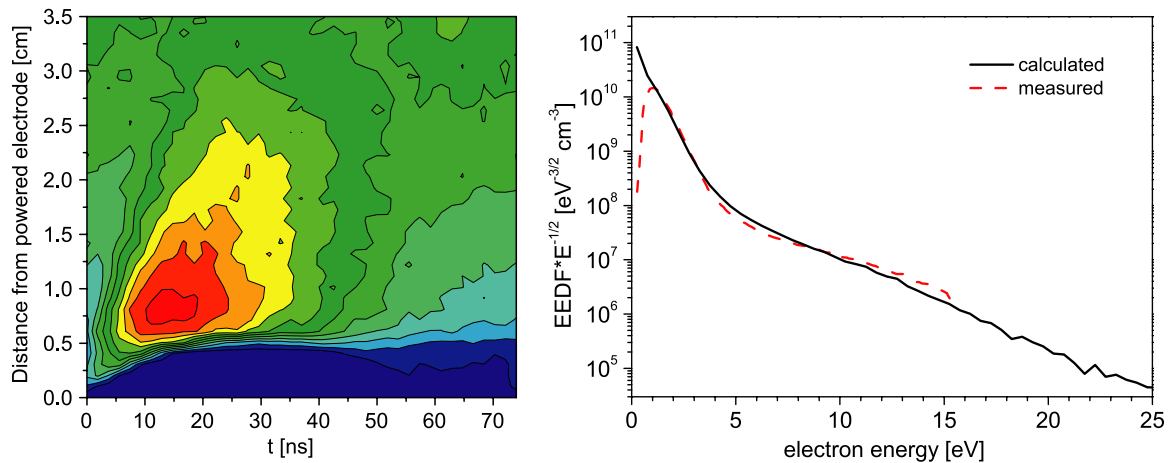


Figure 4. Left: time and space resolved integral of the EEDF above 12 eV as obtained from a Monte Carlo simulation in argon at 2.7 Pa using input parameters from [5]. Right: comparison between measured (figure 18 in [5]) and calculated EEDF under these conditions. (Colour online.)

directed drift velocity, which is of the same order as or higher than the thermal spread of the distribution function.

Electron beams are also observed in the simulation by integrating the EEDF above the threshold energy of the Kr 2p₅ state of about 12 eV (figure 4). Although the qualitative agreement with the experimental observation (figure 3) is very satisfying, a quantitative comparison is difficult. The simulation is inherently one dimensional, while the geometry of the experiment is two dimensional. Therefore, data from an effectively one-dimensional experiment performed by Godyak are used for a direct comparison of the EEDFs in figure 4 ($p = 2.7$ Pa, $n_e = 4.06 \times 10^{10} \text{ cm}^{-3}$, $T_e = 0.74$ eV, $d = 6.7$ cm, $j = 3 \text{ mA cm}^{-2}$ [5]). The simulation reproduces the experimentally obtained EEDF well and, therefore, yields realistic results [9]. It should be noted that using experimental data from the same source at different discharge conditions yields similarly good agreement throughout. In the simulation interaction between charged particles is excluded. This strongly supports the hypothesis of electron beams in comparison with wave effects. Electron beams have been predicted theoretically in PIC simulations before [11, 12].

Under the experimental conditions investigated here the plasma series resonance (PSR) effect plays an important role [10, 13–16]. It leads to high frequency oscillations of the RF current and to a faster initial sheath expansion. This faster expansion of the sheath enhances the generation of beams of highly energetic electrons at the very beginning of the sheath expansion as is clearly visible in figure 3.

Reflections of electron beams at the opposing plasma boundary are observed at lower pressures. Figure 5 shows a spatio-temporal contour plot of the excitation into Ne 2p₁ (19 eV) in an asymmetric CCRF discharge at 0.2 Pa and 8 W in a krypton (90%)–neon (10%) mixture. Under these conditions the electron mean free path (about 7 cm for 12 eV electrons) is long enough to allow electrons to propagate through the discharge several times. At the beginning of the RF cycle a beam of energetic electrons is generated by the expanding sheath. These electrons propagate through the entire bulk,

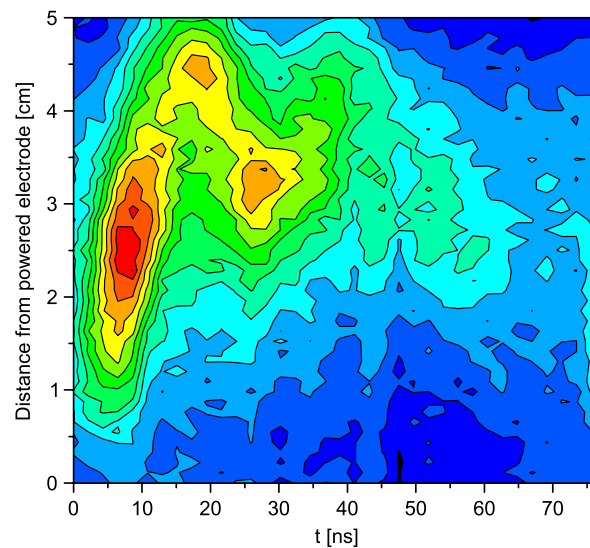


Figure 5. Spatio-temporal plot of the excitation into Ne 2p₁ in an asymmetric CCRF discharge at 0.2 Pa and 8 W in a krypton (90%)–neon (10%) mixture. (Colour online.)

while the sheath is further expanding, until they hit the opposing quartz cylinder. This cylinder acts as a floating surface and charges up negatively, as it is bombarded by energetic electrons. Consequently, a sheath develops in front of the quartz that reflects following electrons back into the plasma. The reflected electrons hit the fully expanded sheath at the powered electrode ($s \approx 2.5$ cm), where they are reflected back into the bulk again. These reflections have been observed theoretically before in PIC and Monte Carlo simulations [12], but have never been detected experimentally until now. This ‘electron ping pong’ effect is supposed to lead to an effective heating of the plasma at low pressures, since the high energy of the beam electrons is deposited in the plasma to a great extent. In principle the same effect occurs in symmetric CCRF discharge, if the electron mean free path is long enough [12]. However, in symmetric discharges PSR oscillations are not possible in the quadratic approximation [16]. Only much smaller contributions by higher terms of odd order might be possible. The

sheath expansion and the related beam velocity are, therefore, expected to be lower. Maxima of the excitation are observed at the positions where the beam is reflected, since incoming and reflected beams overlap at these positions. After some time the beam diverges and is no longer observed in the spatio-temporal plots of the excitation. This is probably caused by collisions and dephasing of faster and slower electrons in the beam.

Finally, the time averaged isotropic EEDF in the bulk is measured by a Langmuir probe in krypton at 1 Pa (figure 6). It shows a bi-Maxwellian shape typical of CCRF discharges at low pressures. The high energy tail is enhanced by stochastic heating [5]. It is reproduced qualitatively by an analytical model (figure 6), that takes into account the influence of a beam of energetic electrons, that is generated during a short fraction of the RF cycle ($\tau/T = 0.15$). As this model is strongly simplified and does not consider various processes such as confinement of energetic electrons, it must not be expected to reproduce experimental results quantitatively. Further, we are aware of the fact that probe measurements of strongly anisotropic distribution functions are not uncritical. In this model the overall EEDF is assumed to be the sum of a time independent isotropic part f_0 , an anisotropic part f_1 attributed to the ohmic current (two-term approximation) and a beam

part f_{beam} :

$$f = f_0 + f_1 \cos \theta + f_{\text{beam}} \quad \text{with } \cos \theta = \frac{v_z}{v}. \quad (1)$$

For f_{beam} , a shifted Maxwellian shape is assumed:

$$f_{\text{beam}}(\vec{v}) = \alpha f_0 [(\vec{v} - \vec{u})^2] \Theta(\vec{v} \cdot \vec{u}), \quad (2)$$

with the Heaviside function $\Theta(\vec{v} \cdot \vec{u})$, considering only positive electron velocities, and $\alpha = n_s/n_0$, where n_s is the electron density in the collapsed sheath and n_0 the density in the bulk ($n_s \ll n_0$). All velocities are normalized to the thermal velocity. \vec{u} is a normalized drift velocity corresponding to twice the sheath velocity [1]. In order to reproduce the measured EEDF, the beam part is averaged over the full solid angle and the EEDF is time averaged using experimentally determined input parameters. As a reasonable analytical approximation u is assumed to be a constant u_0 for $0 \leq t \leq \tau = 11$ ns and zero otherwise. The result is

$$\langle f \rangle = f_0(v^2)(1 + \alpha h(v)), \quad (3)$$

$$h(v) = 1 + \frac{\tau}{T} \left(e^{-u_0^2} \frac{e^{2vu_0} - 1}{2vu_0} - 1 \right). \quad (4)$$

Under the conditions discussed here (krypton discharge, 1 Pa, 8 W) typical values for the input parameters for this model can be estimated based on experimental results applying various diagnostics: the ion density n_s at the electrode is known from the electric field measurements [10] to be $n_s \approx 4 \times 10^8 \text{ cm}^{-3}$. $n_0 \approx 2 \times 10^9 \text{ cm}^{-3}$ is known from Langmuir probe measurements ($\rightarrow \alpha \approx 0.2$). $\tau/T \approx 0.15$ is known from PROES and current measurements [10]. The beam velocity is estimated based on the PROES measurements to be $2.2 \times 10^6 \text{ m s}^{-1}$. The thermal velocity is known from the electron temperature of the cold electrons measured by a Langmuir probe $kT_{e,\text{cold}} \approx 2.3 \text{ eV}$ ($\rightarrow u_0 \approx 2.5$). Figure 7 shows the time averaged EEDF as it results from the model assuming two different beam velocities $u_0 = 1$ and $u_0 = 2.5$. An enhancement of the tail is observed only for $u_0 > 1$, i.e. for beam velocities exceeding the thermal velocity of the cold bulk electrons. This result clearly shows that the nature of

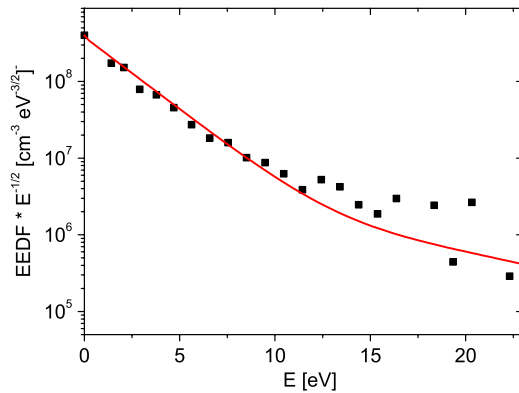


Figure 6. Comparison between an experimentally obtained EEDF in the bulk (points) and a theoretically calculated EEDF (solid line) using a simple analytical model.

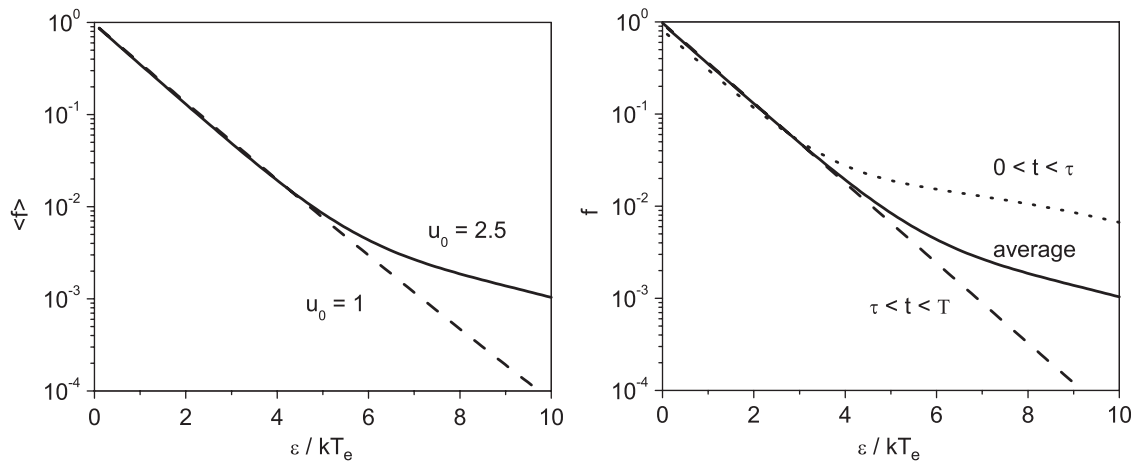


Figure 7. Left: analytically calculated time averaged isotropic EEDF for two different beam velocities. Right: EEDF at two different time intervals and time averaged ($u_0 = 2.5$).

stochastic heating is closely related to electron beams. Figure 7 also shows the temporal variation of the EEDF resulting from this model. As the scattering of the beam is neglected here, the EEDF only deviates from a Maxwellian shape during the fraction of the RF cycle, when the beam propagates.

Acknowledgment

This project is funded by the DFG (SFB 591, GRK 1051) and supported by Andor Technology.

References

- [1] Lieberman M A and Godyak V A 1998 *IEEE Trans. Plasma Sci.* **26** 955
- [2] Surendra M and Graves D B 1991 *Phys. Rev. Lett.* **66** 1469
- [3] Gozadinos G, Turner M M and Vender D 2001 *Phys. Rev. Lett.* **87** 135004
- [4] Kaganovich I D, Polomarov O V and Theodosiou C E 2006 *IEEE Trans. Plasma Sci.* **34** 696
- [5] Godyak V A, Piejak R B and Alexandrovich B M 1992 *Plasma Sources Sci. Technol.* **1** 36–58
- [6] Mahony C M O and Graham W G 1999 *IEEE Trans. Plasma Sci.* **27** 72
- [7] Kampschulte T, Schulze J, Luggenhölscher D, Bowden M D and Czarnetzki U 2007 *New J. Phys.* **9** 18
- [8] Brinkmann R P 2007 *J. Appl. Phys.* **102** 093303
- [9] Heil B, Schulze J, Luggenhölscher D, Czarnetzki U, Mussenbrock T and Brinkmann R P 2007 *Bull. Am. Phys. Soc.* **52** 4
- [10] Schulze J, Kampschulte T, Luggenhölscher D and Czarnetzki U 2007 *J. Phys.: Conf. Ser.* **86** 012010
- [11] Vender D and Boswell R W 1992 *J. Vac. Sci. Technol. A* **10** 1331
- [12] Wood B P 1991 *PhD Thesis* University of Berkeley, CA
- [13] Mussenbrock T and Brinkmann R P 2006 *Appl. Phys. Lett.* **88** 151503
- [14] Mussenbrock T and Brinkmann R P 2007 *Plasma Sources Sci. Technol.* **16** 377–85
- [15] O'Connell D, Gans T, Vender D, Czarnetzki U and Boswell R 2007 *Phys. Plasmas* **14** 034505
- [16] Czarnetzki U, Mussenbrock T and Brinkmann R P 2006 *Phys. Plasmas* **13** 123503